DOI: 10.1002/chem.200900025

Nucleic Acid Templated Reactions: Consequences of Probe Reactivity and Readout Strategy for Amplified Signaling and Sequence Selectivity

Tom N. Grossmann and Oliver Seitz*[a]

Abstract: DNA- and RNA-templated chemical reactions can serve as a diagnostic means for the detection of nucleic acids. Reaction schemes that allow amplified detection are of high interest for polymerase chain reaction (PCR)-free DNA and RNA diagnosis. These reactions typically draw upon the catalytic activity of the template, which is able to trigger the conversion of many signaling molecules per template molecule. However, the design of reactive probes that allow both sensitive and selective nucleic acid detection is a challenge and requires insight into three major parameters: a) reactivity of functional groups involved, b) affinity of probes for the template, and c) the readout system. In this study we used peptide nucleic acid (PNA)-based probes to investigate in detail the signaling power and the selectivity of a transfer reaction derived from a native chemical ligation. We show that subtle variations of the thioesters involved had a tremendous impact on the sensitivity and selectivity of the reaction system. The results suggest that reactions at turnover conditions require low rates of non-templated reaction pathways to provide high target selectivity and sensitivity. On the other hand, very high rates of templated reactions should be avoided to allow mismatched probe–template complexes to dissociate prior to bond formation. Furthermore, the temperature dependence of the DNA-catalyzed transfer reaction was studied and provided insight into crucial strand-exchange processes. Further improvements of selective signaling were achieved through a new readout based on pyrene-transfer reactions. This method reduces background signals and enables significant increases in the signaling rates compared with previous fluorescence-based methods.

Keywords: catalysis · DNA detection · DNA-templated reactions · fluorescence · single-base mutations

Introduction

Nucleic acid templated reactions represent a general tool to control the reactivity of modified oligonucleotides.[1–3] Nucleic acid templates bind reactant oligonucleotides through Watson–Crick base pairing and align their reactive groups. Thereby, the effective molarity is increased, which results in acceleration of a templated reaction. This approach allows fast and selective reactions at very low reactant concentrations compared with conventional synthesis. These features support the use of templated reactions in nucleic acid detection in which product formation indicates the presence of the target structure.[2,3] Several chemical reactions have been used in a DNA- or RNA-templated fashion, including organic reactions such as ligation,[4–11] extension,[12,13] cleavage,[14–18] and transfer[19–21] reactions as well as organometal approaches.[22–24]

The work in the field of nucleic acid diagnostics addresses two major issues, selectivity and sensitivity. High sequence selectivity is required in the detection of acquired single-base mutations. High sensitivity is desired when the target is present at low concentrations. It has been shown that templated chemical reactions can proceed with a very high sequence selectivity that rivals those of the most selective enzymes.[8] By contrast, the sensitivity of most of the available detection chemistries is lagging behind enzymatic methods. Recently, amplified chemical detection systems have been introduced.[3] These reaction systems draw upon the catalytic activity of the template, which allows significant increases in the sensitivity. However, the design of reactive probes that allow the catalytic conversion by the template is a challenge and requires a detailed insight into the reaction rates and strand-exchange processes. We noticed that the influence of these key parameters on selectivity and sensitivity of the

[a] Dr. T. N. Grossmann, Prof. Dr. O. Seitz
Institut für Chemie der Humboldt-Universität zu Berlin
Brook-Taylor-Strasse 2, 12489 Berlin (Germany)
Fax: (+49) 30-2093-7266
E-mail: oliver.seitz@chemie.hu-berlin.de

Supporting information for this article is available on the WWW under http://dx.doi.org/10.1002/chem.200900025.

templated reactions has not been studied previously in detail. This is surprising as these factors can be readily adjusted by reaction design and temperature.

The performance of DNA- and RNA-templated reactions is determined to a large extent by three factors; a) orientation and reactivity of functional groups, b) affinity of the probes for the target, and c) the readout system. Orientation and reactivity of functional groups determine the reaction rates measured in both the presence and absence of the template. Low rates of non-templated background reactions are mandatory for obtaining high target selectivity and sensitivity. In this investigation, we provide evidence that very high rates of templated reactions should be avoided to allow transiently formed mismatched probe-template complexes to dissociate prior to bond formation. It is shown that a templated reaction can be tuned to proceed with high rates of accelerations and/or with high sequence selectivity. We also discuss the critical influence of probe affinity, and show that the optimization of temperature is required to ensure complete hybridization of reactant probes without inhibiting subsequent strand-exchange reactions. This issue has often been ignored in previous reports. Furthermore, we demonstrate the importance of the readout system and present a new excimer-based signaling that indicates the formation of products from templated reactions and is insensitive to non-specific background hydrolysis.

Results and Discussion

A variety of parameters influence the capability of a probe set to detect a given target nucleic acid in a selective and sensitive manner. In the following, we applied peptide nucleic acid (PNA)-based probes in a recently introduced template-catalyzed transfer reaction (Scheme 1).[20] PNA is a chemically and biologically stable DNA analogue that combines an increased affinity towards DNA with a hybridization that is highly sequence selective.[25,26] The transfer reaction provides signal amplification through DNA- and RNA-catalyzed transfer of reporter groups and exhibits the highest catalytic activity in a nucleic acid templated reaction reported so far.[20] This catalytic efficiency has enabled the detection of 500 attomol target RNA.[21] In the following, we used PNA probes as a paradigm to examine the influence of reactivity, probe affinity/temperature, as well as readout on selectivity and sensitivity in nucleic acid detection.

The transfer reaction employs a donating PNA probe **1** and an accepting PNA probe **2**, which are designed to hybridize adjacently to the target. Reporter group **R** in donating probe **1** is attached as a thioester. Hybridization triggers a thiol exchange with the isocysteine moiety in accepting probe **2**, which leads to intermediate **4**. By analogy to the native chemical ligation,[27] a subsequent S→N acyl shift yields transfer product **5**. In a dynamic equilibrium, strand-exchange reactions enable replacement of the product probes **3** and **5**, yielding ternary complex **target·1·2**. Previously, we have reported that the transfer reaction rate is influenced by the number (n) of unpaired nucleotides between the reactive groups of probes **1** and **2** (Scheme 1).[21]

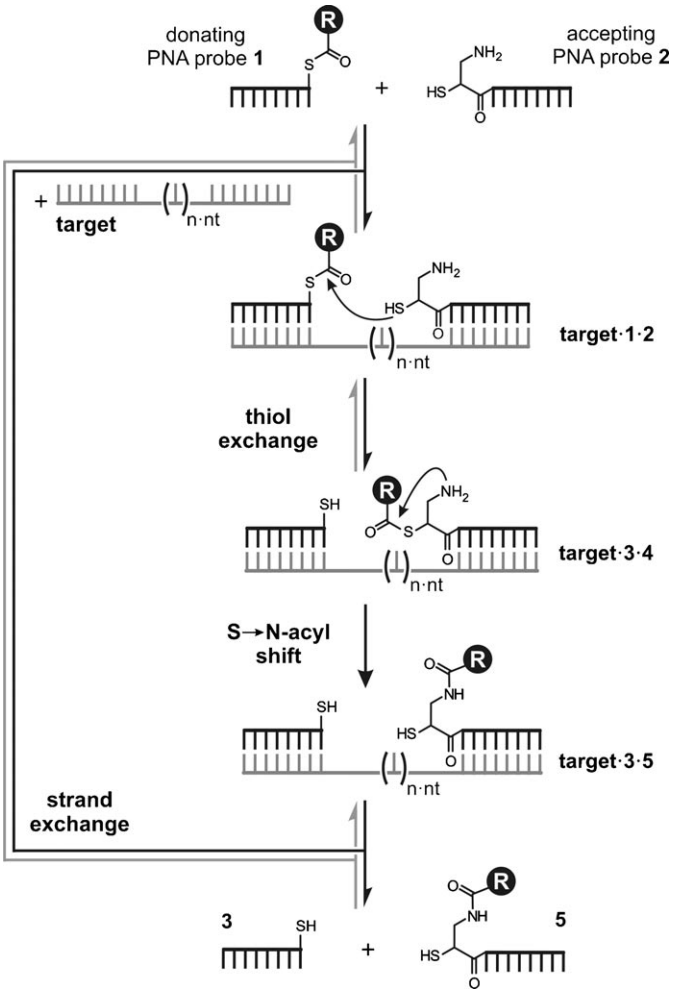

Scheme 1. Catalytic cycle of the nucleic acid catalyzed transfer reaction studied. Reactive probes **1** and **2** are based on PNA (nt = nucleotide).

Thioester reactivity: The rates of native chemical-ligation-like reactions are determined by the reactivity of the 1,2-aminothiol nucleophile and the involved thioesters. In this investigation, the nucleophile (isocysteine–PNA conjugate **8**) was kept constant (Scheme 2a). The isocysteine was chosen as this moiety provided improved rate accelerations in DNA-templated ligation reactions compared with the natural cysteine.[6] Seven thioester derivatives (Scheme 2b, **7a**–**g**, variations of structure **7b** shown in gray boxes) were synthesized (see the Supporting Information). The structural modifications change electrophilicity of the thioester as well as the flexibility of the linker. The template DNA sequences (**RasT** and **RasG**) span a sequence around a known carcinogenic G12 V mutation of the *ras* gene and have been previously used in DNA-templated reactions.[6–8,20,21] Donating and accepting probes were designed to hybridize adjacently to matched target **RasT**, leaving a single nucleotide unpaired between the recognition sequences. The sequence selectivity

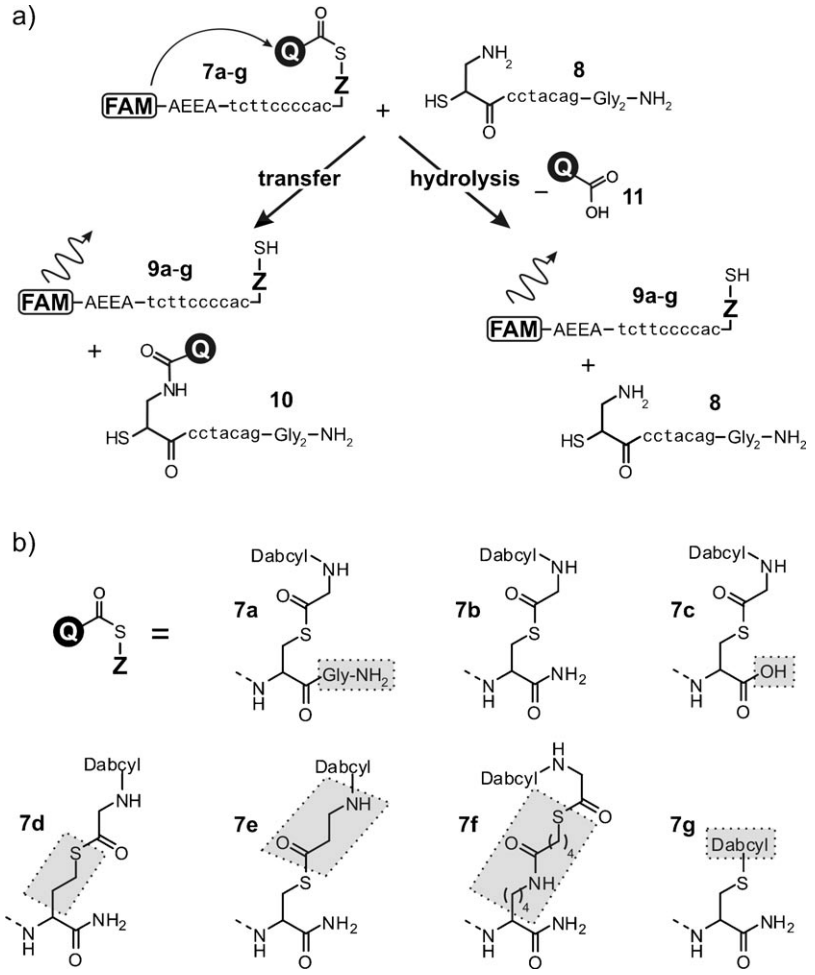

Scheme 2. a) Transfer of a fluorescence quencher (**Q**) from FAM-labeled donating probes **7a**–**g** to non-labeled accepting probe **8** (AEEA = [2-(2-aminoethoxy)ethoxy]acetyl, used target DNA: 3′-TG*AGAAGGGGTGTG-GAXGTC*GCG-5′ (matched **RasT**: X = T; mismatched **RasG**: X = G; recognition sequences shown in italics); b) thioester structures **7a**–**g** (modifications in gray boxes).

was assessed by performing reactions on template **RasG**, which is a DNA sequence that shows a single-base mismatch (G·A) with the PNA sequence of accepting probe **8**.

For facile real-time measurements of probe conversion, we chose the fluorescence-based system depicted in Scheme 2a. Donating probes **7a**–**g** were modified at the N terminus with 6-carboxyfluorescin (FAM). The 4-(4-dimethylaminophenylazo)benzoyl (Dabcyl) served as transferred reporter group **Q**. Dabcyl quenches FAM fluorescence when it is located in close proximity. Two reactions can cause a fluorescence increase: either a transfer of the reporter group (Scheme 2a, left) or hydrolysis of the thioester in donating probes **7a**–**g** (Scheme 2a, right). Each donating probe **7a**–**g** (200 nM) was treated with accepting probe **8** (300 nM) in the presence and absence of target DNA. The background-corrected initial rates with one equivalent (200 nM) of **RasT** ($v_{1\mathbf{RasT}}$, black bars) are given in Figure 1a. In addition, the background-corrected initial rates in the presence of one equivalent (200 nM) of mismatched **RasG** ($v_{1\mathbf{RasG}}$) were determined and used to calculate sequence selectivity ($s = v_{1\mathbf{RasT}}/v_{1\mathbf{RasG}}$, white bars). We observed that the initial rates $v_{1\mathbf{RasT}}$ of the templated reactions differed by one order of magnitude. The highest rates were obtained for glycine-based thioesters **7a** and **7b** that involved rather short linkers. Low transfer rates were determined when benzoyl-type thioesters (**7g**) or long thiol tethers (**7f**) were involved. Of note, a decrease in the reaction rate ($v_{1\mathbf{RasT}}$) was found to result in an increase in sequence selectivity (s), indicating that the rate drops faster with mismatched **RasG** than with matched **RasT**. An explanation for this trend might be that once the donating and the accepting probe are hybridized with matched **RasT**, the transfer reaction occurs before another strand exchange takes place. Owing to the single-base mismatch and the resulting reduced affinity of the accepting probe **8** to **RasG**, only a small percentage of **8** is bound to the template. Presumably, the formed mismatch duplex between **RasG** and **8** exhibits a very short life time. Therefore, dehybridization is fast and able to compete with the transfer reaction. As a result, a reduced transfer reaction rate should favor dehybridization and lead to an even slower reaction on mismatched **RasG** than on matched **RasT**.

Amplified signaling requires that one template molecule induces turnover of many probe molecules. We, thus, investigated the influence of thioester reactivity on the transfer reaction with substoichiometric amounts of **RasT**. Based on the yields of the reactions (**7a**–**g**+**8**) in the presence and absence of target, we calculated the turnover numbers (TON, see the Supporting Information). After 18 h in the presence of 0.01 equivalents (2 nM) of **RasT**, TON ranged from 8 to 38 (Figure 1b). Among all donating probes, **7c** yielded the highest TON (38). Interestingly, the background-corrected initial rate ($v_{0.01\mathbf{RasT}}$, black bars) of this reaction (**7c**+**8**) is about half of the fastest reaction (**7a**+**8**). To explain this observation, one has to consider that the DNA-templated reaction of **7c**+**8** shows the highest rate of acceleration ($a = v_{0.01\mathbf{RasT}+\mathrm{BG}}/v_{\mathrm{BG}}$, gray bars). Owing to this fact, consumption of reactant probe **7c** by background reactions is slow (11% after 18 h). Both donating probes **7a** and **7b** showed higher background reactivity (50% and 40%, respectively, after

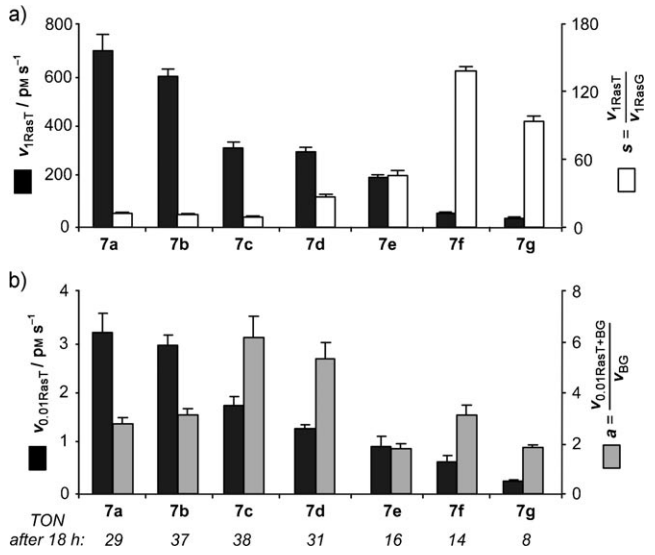

Figure 1. a) Initial rates in the presence of one equivalent of **RasT** (200 nM, black) and corresponding sequence selectivities (white; mean values of two runs, errors represent the range of the data points). b) Initial rates (black) with corresponding rate accelerations (gray; mean values of a triplicate of runs, errors represent 1σ) as well as turnover numbers (TON) after 18 h in the presence of 0.01 equivalents (2 nM) of **RasT** (Conditions: 200 nM **7a**–**g**, 300 nM **8**, 10 mM NaH_2PO_4, 100 mM NaCl, 2 mM triscarboxyethylphosphine, pH 7, 25 °C).

18 h) resulting in more-rapidly decreased reactant concentrations. Therefore, non-templated reactions compete with templated reactions to reduce the TON of the latter systems.

In summary, these investigations show that **RasT** exhibits the highest turnover with the probe set **7c**+**8** and that probe set **7f**+**8** provides the highest sequence selectivity. To study these two systems in detail, we used a more-advanced readout strategy (Scheme 3) that used 5-carboxytetramethylrhodamine (TMR)-modified accepting probe **12** instead of probe **8**. Owing to this modification, it is possible to distinguish between the selective transfer reaction (Scheme 3, left) and the unselective hydrolysis (Scheme 3, right). Upon transfer of the Dabcyl group (**Q**) FAM fluorescence is activated, whereas TMR fluorescence is quenched. On the contrary, hydrolysis of the thioester bond increases FAM fluorescence without affecting TMR fluorescence.

Using this setup, it was possible to determine the contribution of the non-templated transfer reaction ($v_{BG(tr)}$) to the total background ($v_{BG(tot)}$). Measurements of the TMR emission provide the rate acceleration of the transfer reaction ($a_{tr} = v_{0.01\mathbf{RasT}+BG(tr)}/v_{BG(tr)}$) and measurements of the FAM emission can be used to quantify the acceleration of total probe conversion ($a_{tot} = v_{0.01\mathbf{RasT}+BG(tot)}/v_{BG(tot)}$, for details see the Supporting Information). For both probe sets, less than 20% of background conversion is caused by the transfer reaction (Table 1, no DNA). This means that thioester hydrolysis is the major pathway of non-templated background reactions. In addition, background-corrected initial rates in the presence of matched **RasT** and mismatched **RasG** (Table 1) were calculated. As observed when combined with accepting probe **8**, donating probe **7c** shows higher reactivity than **7f** in the presence of **RasT**. Based on these data, rate accelerations upon the addition of one equivalent of **RasT** were determined (Figure 2a). The transfer reaction was accelerated (a_{tr}) by a factor of 1720 for **7c** and by a factor of 980 for **7f**. Taking the total background reaction into account, the rate acceleration (a_{tot}) reduces to 323 and 113, respectively (Figure 2a). This indicates that a readout that is specific for product formation rather than probe conversion should allow for improved signaling as it reduces the background signal.

Table 1. Initial rates ($pM s^{-1}$, mean values of two runs) of the reaction of **7c/f** with **12** in the presence of one equivalent (200 nM) and 0.1 equivalents (20 nM) of **RasT** and **RasG**, respectively.[a]

	no DNA $v_{BG(tr)}$ ($v_{BG(tot)}$)	1/0.1 equiv **RasT** $v_{1\mathbf{RasT}}/v_{0.1\mathbf{RasT}}$	1/0.1 equiv **RasG** $v_{1\mathbf{RasG}}/v_{0.1\mathbf{RasG}}$
7c+**12**	2.42×10^{-1} (1.29)	416/73.8	13.2/1.70
7f+**12**	6.26×10^{-2} (5.46×10^{-1})	61.3/7.53	$2.01\times10^{-1}/2.05\times10^{-2}$

[a] Conditions: 200 nM **7c/f**, 200 nM **12**, 10 mM NaH_2PO_4, 200 mM NaCl, 0.2 mM triscarboxyethylphosphine, 0.1 $g L^{-1}$ Roche blocking reagent, pH 7, 37 °C.

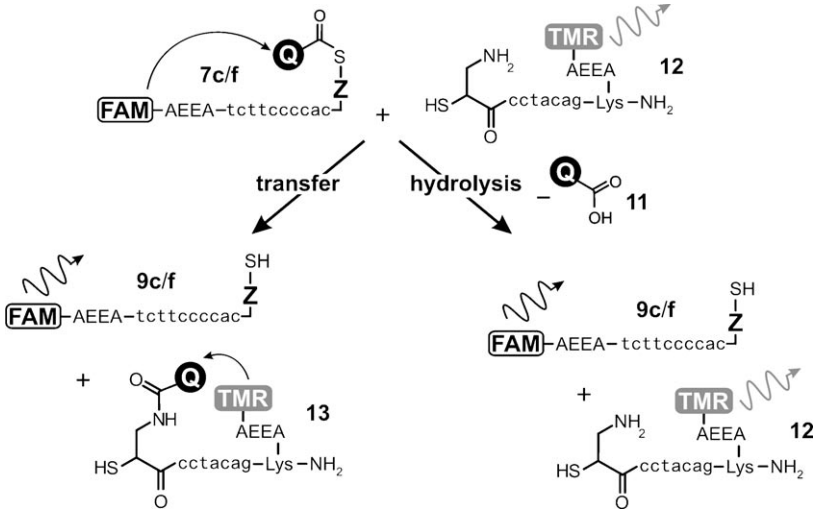

Scheme 3. Transfer of a fluorescence quencher (**Q**) from FAM-labeled donating probes **7c** and **7f** to TMR-labeled accepting probe **12** (AEEA = [2-(2-aminoethoxy)ethoxy]acetyl, used target DNA: 3′-TG*A*-*GAAGGGGTGTGGAXGTC*GCG-5′ (matched **RasT**: X = T; mismatched **RasG**: X = G; recognition sequences shown in italics).

Figure 2b gives sequence selectivities of the reaction of donating probes **7c** and **7f** with

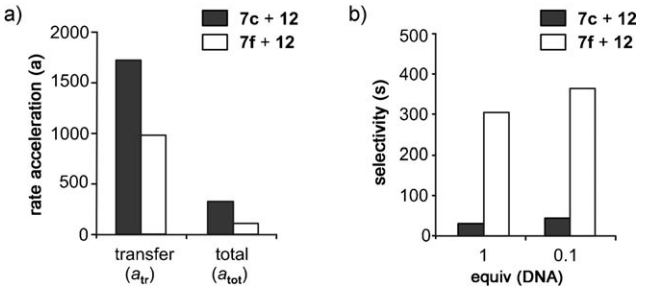

Figure 2. a) Rate accelerations ($a_{tr}=v_{1\mathbf{RasT}+BG(tr)}/v_{BG(tr)}$ and $a_{tot}=v_{1\mathbf{RasT}+BG(tot)}/v_{BG(tot)}$) as well as b) sequence selectivity ($s=v_{X\mathbf{RasT}}/v_{X\mathbf{RasG}}$) based on data in Table 1.

accepting probe **12** in presence of one equivalent (200 nM) and 0.1 equivalents (20 nM) of DNA. The data confirm the excellent single-mismatch discrimination of donating probe **7f**. In presence of 0.1 equivalents of DNA, a selectivity of $s=367$ was achieved. Under the same conditions, we observed a value of $s=44$ for donating probe **7c**. This exceeds the selectivities that were observed in the previous screening (Figure 1a). The explanation for this behavior is the increase in the reaction temperature from 25°C to 37°C, which results in a more selective hybridization.

Probe affinity adjusted by temperature and concentration: The turnover numbers that can be achieved in nucleic acid catalyzed reactions depend on probe affinity; more precisely on the rate of starting probe association and product probe dissociation. For a given probe set, these exchange rates can readily be adjusted by temperature and probe concentration. Thus, further studies focused on optimizing the temperature for high catalytic activity of the DNA template **RasT** in the transfer reaction. We decided to use probe set **7c+12** for these studies as it represents the most active substrate among the thioesters studied. Donating probe **7c** and accepting probe **12** were allowed to react at 200 nM concentration each. In absence of DNA, the initial rate of the total background ($v_{BG(tot)}$) increased with temperature from 0.52 pM s^{-1} at 25°C to 2.46 pM s^{-1} at 45°C (Figure 3a). The

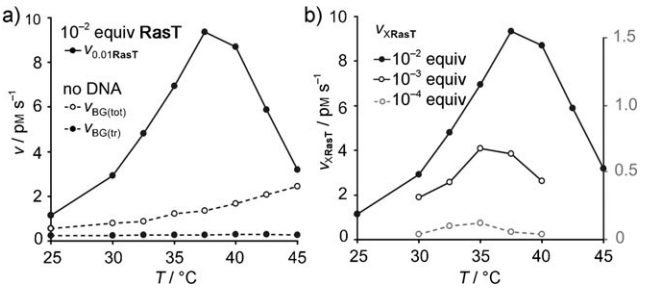

Figure 3. a) Temperature dependence of initial rates in the presence of 0.01 equivalents (2 nM) of **RasT** ($v_{0.01RasT}$, background corrected) as well as rates of background reactions; b) temperature dependence of initial rates in the presence of 10^{-2} (2 nM), 10^{-3} (0.2 nM) and 10^{-4} equivalents (0.02 nM) of **RasT** (mean values of two runs; conditions: 200 nM **7c**, 200 nM **12**, 10 mM NaH_2PO_4, 200 mM NaCl, 1 mM triscarboxyethylphosphine, 0.1 g L^{-1} Roche blocking reagent, pH 7).

background transfer reaction ($v_{BG(tr)}$) alone showed less temperature dependence with initial rates between 0.24 and 0.29 pM s^{-1}. This indicates that the increases in background signals are predominantly caused by hydrolysis. In the presence of 0.01 equivalents (2 nM) of **RasT**, background-corrected initial rates ($v_{0.01RasT}$) increase with temperature between 25 and 37.5°C (Figure 3a). Above 40°C, transfer rates decrease with increasing temperature. An explanation for the rise in catalytic activity up to 37.5°C is the acceleration of strand exchange, which fosters turnover in the cycle depicted in Scheme 1. However, the amount of hybridized probes decreases as temperature increases, causing less efficient catalysis above 40°C. The melting temperatures of **7c** and **12** with **RasT** at 1 μM duplex concentration were 46°C for both probes (see the Supporting Information). Taking into account that duplex stability decreases with reduced concentration,[28] the optimum of the catalytic activity (37.5–40°C) at a **RasT** concentration of 2 nM is in the range of the observed melting temperatures. This observation suggests that strand-exchange processes are rate limiting at these conditions. Reducing the **RasT** concentration from 2 nM (10^{-2} equiv) to 0.2 nM (10^{-3} equiv) and 0.02 nM (10^{-4} equiv) results in the background-corrected initial rates that are given in Figure 3b. The optimum for high catalytic activity is shifted to a lower temperature (from ~38°C to ~35°C) when the template load is reduced from 10^{-2} to 10^{-4} equivalents of **RasT**. This behavior is most likely caused by the concentration dependence of the melting temperature.[28]

An appropriate temperature for the detection of low **RasT** concentrations with probe set **7c+12** (200 nM each) is 35°C. Figure 4a shows the time courses of the ratio of the

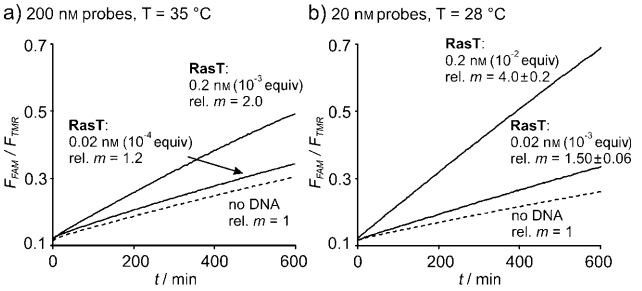

Figure 4. Time courses of FAM/TMR ratio with relative slopes (rel. *m*) that set *m* in the absence of DNA to 1 for a) 200 nM and b) 20 nM concentration of each **7c** and **12**. For the concentration of 20 nM, a triplicate of runs was performed. Errors of rel. *m* (**RasT**) include the propagated errors of the no-template control reaction (no DNA). Conditions: 10 mM NaH_2PO_4, 200 mM NaCl, 1 mM triscarboxyethylphosphine, 0.1 g L^{-1} Roche blocking reagent, pH 7.

increasing FAM emission and the decreasing TMR emission (F_{FAM}/F_{TMR}, see Scheme 3) at this temperature. The measurements were performed in the absence (no DNA) and the presence of 0.2 nM (10^{-3} equiv) as well as 0.02 nM (10^{-4} equiv) **RasT.** Upon addition of **RasT**, the slope (*m*) of the signal was increased by a factor of 2.0 and 1.2, respectively. An improvement in signaling was achieved when the

probe concentration was reduced from 200 nM to 20 nM. To calculate errors in reproducibility, triplicate runs were performed. In addition, 28 °C was chosen as the reaction temperature to ensure hybridization of the probes with the target. Under these conditions the background signal was slightly reduced (Figure 4b). In the presence of 0.2 nM (10^{-2} equiv) and 0.02 nM (10^{-3} equiv) **RasT**, the slope (m) of the signal increased by a factor of 4.0 ± 0.2 and 1.50 ± 0.06, respectively.

It is instructive to compare the signal output provided by our transfer reaction with the signal output provided by current state-of-the art hybridization probes such as molecular beacons (MB).[29,30] In the absence of target, MBs form a stem–loop structure, which is opened upon hybridization with the target. This structural rearrangement triggers the activation of, for example, a fluorescent signal. Each target molecule is capable of activating a single MB. This prevents signal amplification. A very sensitive approach allowed the detection of 0.17 nM target DNA in the presence of 100 nM MB.[31] The maximum 22-fold signal increase at 1:1 stoichiometry decreases to a factor of approximately 1.04 at the 588-fold excess of MB for 0.17 nM target. The comparison with the catalyzed transfer of a reporter group (signal increase of 1.50 ± 0.06 with only 0.02 nM target) highlights the advantages of signal amplification.

Readout strategies: An important issue for the design of a probe set is the readout system. So far, we have described reactions based on the transfer of a fluorescence quencher. Although high turnover numbers were demonstrated,[20] the problem of background signals was not appropriately addressed as both the target-dependent transfer reaction and the target-independent hydrolysis provided a positive fluorescence signal (FAM, Scheme 2 and Scheme 3). Therefore, we set out to explore the transfer of a group that enables the specific detection of transfer products only. In a paradigm study for a hydrolysis-insensitive readout, the transfer of a pyrene (Py) reporter (Scheme 4) from donating PNA probe **14** to accepting PNA probe **15** was investigated. Accepting probe **15** bears an additional C-terminal Py group. Specific readout of the transfer is achieved by monitoring the excimer signal that is produced as the result of the interactions between the two pyrene groups[32–34] in the transfer product **17** (Scheme 4, left). Hydrolysis of the thioester bond in **14** does not induce excimer formation (Scheme 4, right).

To allow a direct comparison with the transfer of a fluorescence quencher, probe structures and PNA sequences were derived from probe set **7c+12**. The length of the PNA sequence of donating probe **14** was reduced by two nucleotides to compensate for the effect of the FAM label in probe **7c**, which is known to reduce duplex stability.[35] Figure 5a shows the fluorescence spectra at the beginning of the reaction of probes **14** and **15** (dashed line), as well as after 30 min in the presence of one equivalent of matched **RasT** (black line) and single-base mismatched **RasG** (gray line). Intensive excimer fluorescence with a maximum at 480 nm was only observed in the presence of **RasT**. Kinetic measurements of the excimer fluorescence (see the Supporting Information) showed a 23-fold enhancement after 1 hour in the presence of one equivalent of **RasT**.

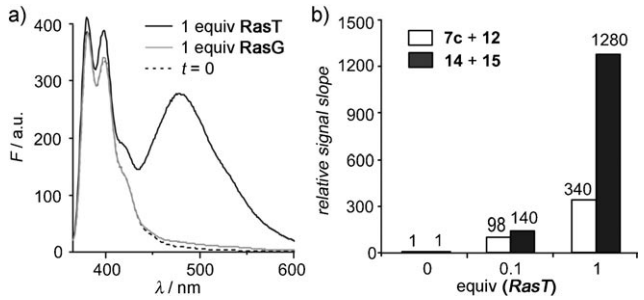

Figure 5. a) Fluorescence spectra ($\lambda_{ex} = 340$ nm) of the reaction of donating probe **14** and accepting probe **15** at $t = 0$ and after 30 min in the presence of one equivalent (200 nM) of **RasT** and **RasG** (conditions: 200 nM **14**, 200 nM **15**, 10 mM NaH_2PO_4, 200 mM NaCl, 0.2 mM triscarboxyethylphosphine, 0.1 g L^{-1} Roche blocking reagent, pH 7, 37 °C); b) relative slope of the signal (F_{FAM}/F_{TMR} for **7c+12**; F_{Py} for **14+15**) upon addition of one equivalent (200 nM) and 0.1 equivalents (20 nM) of **RasT**, respectively.

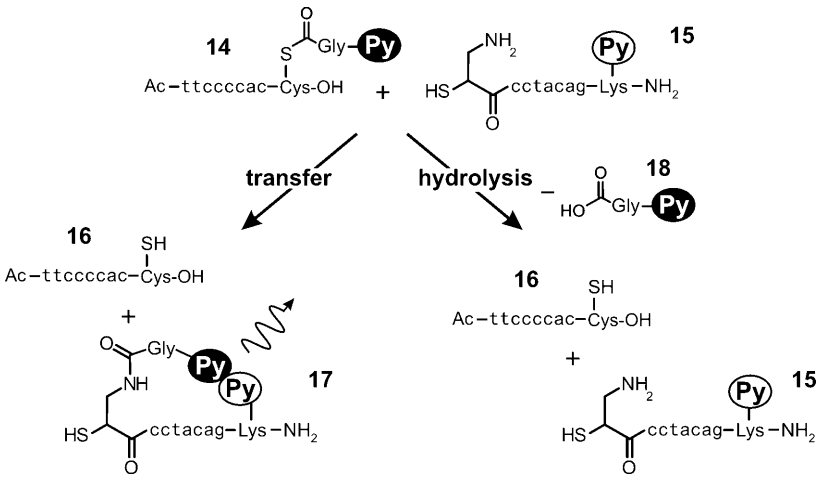

Scheme 4. Transfer of a pyrene group (Py = pyrenebutyryl) from donating probe **14** to Py-labeled accepting probe **15**, used target DNA: 3′-TGAG*AAGGGGTGTGGAXGTC*GCG-5′ (matched **RasT**: X = T; mismatched **RasG**: X = G; recognition sequences shown in italics).

Based on the kinetic measurements, initial rates were calculated. Owing to the readout system, only the transfer background reaction is detectable through excimer fluorescence in the absence of DNA. The corresponding initial rate ($v_{BG(tr)} = 1.2 \times 10^{-1}$ pM s^{-1}) lies in the

range of the transfer rate observed for **7c+12** (Table 1). With one equivalent (200 nM) probes, the rate of pyrene transfer was 44-fold higher on matched target **RasT** ($v_{1\mathbf{RasT}}$ = 157 pM s^{-1}) than on mismatched **RasG** ($v_{1\mathbf{RasG}}$ = 3.5 pM s^{-1}). Substoichiometric amounts of **RasT** also proved efficient in furnishing rapid enhancements of the excimer signal ($v_{0.1\mathbf{RasT}}$ = 17.2 pM s^{-1}). In the presence of 0.1 equivalents (20 nM) of target DNA, the selectivity increased to s = 67. This exceeds the selectivity obtained in the reaction of **7c** with **12** (Figure 2b). Figure 5b compares the relative slopes of the signal achieved upon excimer formation (**14+15**, black) with the one determined by monitoring the F_{FAM}/F_{TMR} ratio (Dabcyl transfer: **7c+12**, white). The presence of 0.1 equivalents of **RasT** accelerated the excimer signaling by a factor of 140, which exceeds the 98-fold acceleration of the F_{FAM}/F_{TMR} signal. The addition of one equivalent of **RasT** triggers higher accelerations of signaling rates. Under these conditions, excimer signaling surpassed F_{FAM}/F_{TMR} signaling by a factor of four. The DNA-catalyzed transfer of a pyrene reporter is the first transfer reaction that triggers the activation of a fluorescence signal that is insensitive to nonspecific background hydrolysis. Therefore, the background signal is lowered significantly.

Conclusions

We used the transfer of a reporter group, a reaction that follows the mechanism of the native chemical ligation, as a model system for a DNA-templated reaction. We demonstrated the influence of important reaction parameters such as a) reactivity of functional groups, b) affinity of probes for the target, and c) the readout system on sensitivity and selectivity of the DNA-catalyzed reaction. For the modulation of the thioester reactivity, fluorescence-based real-time measurements exposed a general trend. Decreases in the reaction rate on the target resulted in increased sequence selectivity. Based on these experiments, we identified specialized probe sets that either provide very high turnover numbers or very high sequence selectivity.

A more elaborated readout system, in which transfer of the Dabcyl quencher triggered the activation of fluorescein fluorescence and the quenching of rhodamine fluorescence, allowed a clear distinction between selective transfer reactions and unselective hydrolysis reactions. We used this system to assess how changes of the affinity of the probes for the template influence the template-catalyzed reaction. The probe affinity was conveniently adjusted through changes in the reaction temperature. The template-catalyzed reaction proceeded at the highest rates close to the melting temperature of the probe–template duplexes. We assume that the optimum conditions between sufficient template affinity of the probes and effective strand exchange lie close to the melting temperature of the formed duplexes. Our investigations revealed that the signaling power of a given probe set can be improved not only through reaction design but also through adjustment of probe concentration. The improvements in signaling rates observed when the probe concentration was decreased (at constant template concentration) suggest that many previous reactions may have been performed at conditions that provided high levels of background reaction.[4,16,36] Of note, the reduction of probe concentration increases the contribution of the templated reaction and, thereby, increases sensitivity.

The results furthermore demonstrate that the selection of an appropriate readout method can improve selective signaling. We introduced the excimer formation triggered by pyrene transfer as a method that allows the specific detection of the transfer product only. We showed that measurements of excimer fluorescence provided up to fourfold increases in the signaling rates compared with the previously described transfer of a fluorescence quencher from a fluorescein- to a rhodamine-modified probe.

Standard methods for the sequence-selective detection of nucleic acids often employ the use of hybridization probes such as molecular beacons (MB)[29–31] or adjacent probes.[37] These approaches do not enable signal amplification. For highly sensitive detection, hybridization probes are applied in combination with the polymerase chain reaction (PCR). Compared with probes used for target-catalyzed reactions, hybridization probes are more readily accessible and the presence of the target can be detected within a shorter response time. On the other hand, the high sensitivity of target-catalyzed reactions certainly is a valuable asset, which might facilitate the detection of low abundant nucleic acid material as required in PCR-less detection of nucleic acid targets[21] and live-cell RNA analysis.[5]

Experimental Section

Materials and instruments: PNA monomers were purchased from Applied Biosystems. DNA was purchased from BioTeZ Berlin Buch GmbH, Germany, in HPLC quality. Water was purified with a Milli-Q ultra pure water purification system. Automated linear solid-phase synthesis was performed by using an Intavis ResPep parallel synthesizer equipped with micro scale columns for PNA synthesis. For details of probe synthesis, see the Supporting Information. Analytical HPLC was performed with a Merck-Hitachi Elite LaChrom chromatograph (column: Varian Polaris C18 A 5 μ 250×46, pore size 220 Å) at 55 °C. Eluents: A (98.9% H_2O, 1% acetonitrile, 0.1% trifuloroacetic acid (TFA)) and B (98.9% acetonitrile, 1% H_2O, 0.1% TFA) were used in a linear gradient with a flow rate of 1 mL min^{-1} for analytical and 6 mL min^{-1} for semi-preparative HPLC. For probe characterization, MALDI-TOF mass spectra were recorded with a Voyager-DE Pro Biospectrometry workstation of PerSeptive Biosystems.

Fluorescence-based kinetic measurements: Fluorescence spectroscopy was performed by using a Varian Cary Eclipse spectrometer. Measurements were carried out in fluorescence quartz cuvettes (4×10 mm). The buffer solution (10 mM NaH_2PO_4, 100 or 200 mM NaCl, and 0.2–2 mM tris-carboxyethylphosphine) was degassed and the pH value adjusted to 7. To prevent adsorption of TMR- and Py-labeled probes on the glass surface, roche blocking reagent (0.1 g L^{-1}) was added. Subsequent manipulations were carried out while avoiding unnecessary exposure to oxygen. The buffer solution (final volume 1 mL) was placed in a cuvette and accepting probe (**8**, **12** or **15**; 0.02–0.3 nmol) and DNA (**RasT** or **RasG**; if required) were added. After setting the solution to the required temperature, donating probe (**7a–g** or **14**; 0.02–0.2 nmol) were added and the cuvette was

placed in the spectrometer. Initial rates of DNA-catalyzed transfer and background reactions were determined based on the linear phase of the time course.

Melting-temperature (T_M) measurements: UV melting curves were measured at 260 nm by using a Varian Cary 100 spectrometer equipped with a peltier block. A degassed aqueous solution (10 mM NaH_2PO_4, 200 mM NaCl, pH 7) was used as the buffer solution. The DNA **RasT** was mixed with probe **7c** or **12** with a 1:1 stoichiometry. The solutions were adjusted to a final duplex concentration of 1 μM. Prior to analysis, the samples were heated to the maximum temperature of 75 °C and cooled to the starting temperature of 20 °C. Melting curves were recorded at a rate of 0.5 °C min^{-1} (triplicate of runs). T_M values were defined as the maximum of the first derivative of the melting curve.

Acknowledgements

T.N.G. is grateful for a fellowship from the Studienstiftung des deutschen Volkes.

[1] X. Y. Li, D. R. Liu, *Angew. Chem.* **2004**, *116*, 4956–4979; *Angew. Chem. Int. Ed.* **2004**, *43*, 4848–4870.
[2] A. P. Silverman, E. T. Kool, *Chem. Rev.* **2006**, *106*, 3775–3789.
[3] T. N. Grossmann, A. Strohbach, O. Seitz, *ChemBioChem* **2008**, *9*, 2185–2192.
[4] H. Abe, E. T. Kool, *J. Am. Chem. Soc.* **2004**, *126*, 13980–13986.
[5] H. Abe, E. T. Kool, *Proc. Natl. Acad. Sci. USA* **2006**, *103*, 263–268.
[6] C. Dose, S. Ficht, O. Seitz, *Angew. Chem.* **2006**, *118*, 5495–5499; *Angew. Chem. Int. Ed.* **2006**, *45*, 5369–5373.
[7] C. Dose, O. Seitz, *Bioorg. Med. Chem.* **2008**, *16*, 65–77.
[8] S. Ficht, C. Dose, O. Seitz, *ChemBioChem* **2005**, *6*, 2098–2103.
[9] S. Ogasawara, K. Fujimoto, *Angew. Chem.* **2006**, *118*, 4624–4627; *Angew. Chem. Int. Ed.* **2006**, *45*, 4512–4515.
[10] Y. Yoshimura, Y. Noguchi, H. Sato, K. Fujimoto, *ChemBioChem* **2006**, *7*, 598–601.
[11] H. Abe, Y. Kondo, H. Jinmei, N. Abe, K. Furukawa, A. Uchiyama, S. Tsuneda, K. Aikawa, I. Matsumoto, Y. Ito, *Bioconjugate Chem.* **2008**, *19*, 327–333.
[12] N. Griesang, K. Giessler, T. Lommel, C. Richert, *Angew. Chem.* **2006**, *118*, 6290–6294; *Angew. Chem. Int. Ed.* **2006**, *45*, 6144–6148.
[13] M. Röthlingshöfer, E. Kervio, T. Lommel, U. Plutowski, A. Hochgesand, C. Richert, *Angew. Chem.* **2008**, *120*, 6154–6157; *Angew. Chem. Int. Ed.* **2008**, *47*, 6065–6068.
[14] Z. C. Ma, J. S. Taylor, *Proc. Natl. Acad. Sci. USA* **2000**, *97*, 11159–11163.
[15] J. F. Cai, X. X. Li, J. S. Taylor, *Org. Lett.* **2005**, *7*, 751–754.
[16] Z. L. Pianowski, N. Winssinger, *Chem. Commun.* **2007**, 3820–3822.
[17] R. M. Franzini, E. T. Kool, *ChemBioChem* **2008**, *9*, 2981–2988.
[18] K. Furukawa, H. Abe, J. Wang, M. Uda, H. Koshino, S. Tsuneda, Y. Ito, *Org. Biomol. Chem.* **2009**, *7*, 671–677.
[19] J. F. Cai, X. X. Li, X. Yue, J. S. Taylor, *J. Am. Chem. Soc.* **2004**, *126*, 16324–16325.
[20] T. N. Grossmann, O. Seitz, *J. Am. Chem. Soc.* **2006**, *128*, 15596–15597.
[21] T. N. Grossmann, L. Roglin, O. Seitz, *Angew. Chem.* **2008**, *120*, 7228–7231; *Angew. Chem. Int. Ed.* **2008**, *47*, 7119–7122.
[22] J. Brunner, A. Mokhir, R. Kraemer, *J. Am. Chem. Soc.* **2003**, *125*, 12410–12411.
[23] I. Boll, R. Kraemer, J. Brunner, A. Mokhir, *J. Am. Chem. Soc.* **2005**, *127*, 7849–7856.
[24] R. M. Franzini, E. T. Kool, *Org. Lett.* **2008**, *10*, 2935–2938.
[25] P. E. Nielsen, M. Egholm, R. H. Berg, O. Buchardt, *Science* **1991**, *254*, 1497–1500.
[26] E. Uhlmann, A. Peyman, G. Breipohl, D. W. Will, *Angew. Chem.* **1998**, *110*, 2954–2983; *Angew. Chem. Int. Ed.* **1998**, *37*, 2796–2823.
[27] P. E. Dawson, T. W. Muir, I. Clark-Lewis, S. B. H. Kent, *Science* **1994**, *266*, 776–779.
[28] J. SantaLucia, *Proc. Natl. Acad. Sci. USA* **1998**, *95*, 1460–1465.
[29] S. Tyagi, F. R. Kramer, *Nat. Biotechnol.* **1996**, *14*, 303–308.
[30] K. M. Wang, Z. W. Tang, C. Y. J. Yang, Y. M. Kim, X. H. Fang, W. Li, Y. R. Wu, C. D. Medley, Z. H. Cao, J. Li, P. Colon, H. Lin, W. H. Tan, *Angew. Chem.* **2009**, *121*, 870–885; *Angew. Chem. Int. Ed.* **2009**, *48*, 856–870.
[31] P. Zhang, T. Beck, W. H. Tan, *Angew. Chem.* **2001**, *113*, 416–419; *Angew. Chem. Int. Ed.* **2001**, *40*, 402–405.
[32] T. Förster, *Angew. Chem.* **1969**, *81*, 364–374; *Angew. Chem. Int. Ed. Engl.* **1969**, *8*, 333–343.
[33] F. D. Lewis, Y. F. Zhang, R. L. Letsinger, *J. Am. Chem. Soc.* **1997**, *119*, 5451–5452.
[34] K. Yamana, Y. Fukunaga, Y. Ohtani, S. Sato, M. Nakamura, W. J. Kim, T. Akaike, A. Maruyama, *Chem. Commun.* **2005**, 2509–2511.
[35] T. Ratilainen, A. Holmen, E. Tuite, G. Haaima, L. Christensen, P. E. Nielsen, B. Norden, *Biochemistry* **1998**, *37*, 12331–12342.
[36] Z. Tang, A. Marx, *Angew. Chem.* **2007**, *119*, 7436–7439; *Angew. Chem. Int. Ed.* **2007**, *46*, 7297–7300.
[37] R. A. Cardullo, S. Agrawal, C. Flores, P. C. Zamecnik, D. E. Wolf, *Proc. Natl. Acad. Sci. USA* **1988**, *85*, 8790–8794.

Received: January 5, 2009
Revised: March 7, 2009
Published online: June 3, 2009

